THE JOURNAL OF PHYSICAL CHEMISTRY Letters

Letter

Cite This: J. Phys. Chem. Lett. 2018, 9, 874−880

pubs.acs.org/JPCL

Aziridinium Lead Iodide: A Stable, Low-Band-Gap Hybrid Halide Perovskite for Photovoltaics

Chao Zheng* and Oleg Rubel*

Department of Materials Science and Engineering, McMaster University, 1280 Main Street West, Hamilton, Ontario L8S 4L8, Canada

Supporting Information

ABSTRACT: The low ionization energy of an *A* site molecule is a very important factor, which determines the thermodynamical stability of $APbI_3$ hybrid halide perovskites, while the size of the molecule governs the stable phase at room temperature and, eventually, the band gap. It is challenging to achieve both a low ionization energy and the reasonable size for the PbI_3 cage to circumvent the stability issue inherent to hybrid halide perovskites. Here we propose a new three-membered charged ring radical, which demonstrates a low ionization energy that renders a good stability for its corresponding perovskite and a reasonable cation size that translates into a suitable band gap for the photovoltaic application. We use ab initio calculations to evaluate a polymorphism of the crystal structure of the proposed hybrid halide perovskite, its stability, and electronic properties in comparison with the mainstream perovskites, such as the methylammonium and formamidinium lead iodide.

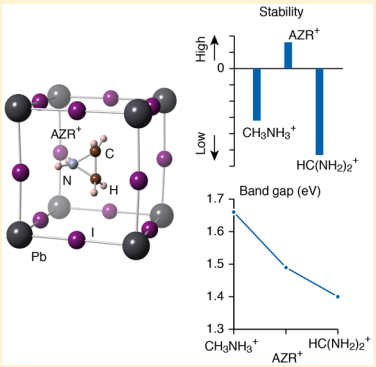

During the past 10 years, hybrid halide perovskites increasingly catch researchers' attention as the absorber layers in photovoltaics.[1−5] Favorable electronic properties and a low-cost fabrication method give hybrid halide perovskites an advantage over the traditional silicon. One drawback of hybrid halide perovskites is their instability. The hybrid halide perovskites easily decompose under the influence of high temperature, oxygen, water, and even UV light.[6−8] Zhang et al.[9] pointed out that the instability of methylammonium (MA) lead iodide is intrinsic due to the similar total energies of the reactant and products obtained from the density functional theory[10] (DFT) calculation. To commercialize the hybrid halide perovskite photovoltaics, the stability issue should be resolved.

The improvements of device architectures are proposed to stabilize the perovskite photovoltaics.[3,11−13] However, the power conversion efficiencies still decrease by 60% of the initial value after 1100 h,[14] which is far from silicon solar panels that come on today's market with a 25-year long performance warranty. The nature of instability of hybrid halide perovskite cannot be eliminated. We propose a new perovskite material with a highly unfavorable decomposition reaction enthalpy, which should stabilize it against degradation.

Hybrid halide perovskite structures discussed here are considered in the form of $APbI_3$. Here *A* stands for an organic cation in the lead iodide framework. On the basis of our recent paper, the ionization energy of the molecule on *A* site (in addition to its size) can be an important factor that determines the stability of perovskites.[15] A lower ionization energy of the cation favors a more stable perovskite structure.

Kieslich et al.[16] proposed nitrogen-based cations, which were not used in perovskites before. From this group, an azetidinium radical $(CH_2)_3NH_2$ is promising due to its compact structure. This four-membered ring cation is larger than MA cation but slightly smaller than the formamidinium $HC(NH_2)_2$. Recently, the azetidinium lead iodide $(CH_2)_3NH_2PbI_3$ was successfully synthesized.[17] The crystal structure of quasicubic $(CH_2)_3NH_2PbI_3$ is shown in Figure 1b. Pering et al.[17] reported that $(CH_2)_3NH_2PbI_3$ demonstrates a very good stability when soaked in water in contrast with the MA lead iodide $CH_3NH_3PbI_3$. This observation correlates with the ionization energy of the $(CH_2)_3NH_2$ radical being 0.4 eV below that of MA. However, the wide band gap of 2.15 eV for $(CH_2)_3NH_2PbI_3$ is not promising for photovoltaics.[17]

Interestingly, there are also three-membered rings,[18] of which the aziridinium radical $(CH_2)_2NH_2$ is a promising candidate to be used as the organic cation at *A* site of hybrid halide perovskites. Figure 1a illustrates a proposed quasicubic phase of $(CH_2)_2NH_2PbI_3$. This three-membered ring cation is only slightly larger than MA. As we will show below, the ionization energy of $(CH_2)_2NH_2$ is also much lower than that of MA. This fact implies that aziridinium lead iodide $(CH_2)_2NH_2PbI_3$ might be stable and suitable for photovoltaic applications. Here we discuss the structural stability and electronic properties of the new perovskite $(CH_2)_2NH_2PbI_3$. We also compare relevant electronic properties between $(CH_2)_2NH_2PbI_3$, $CH_3NH_3PbI_3$, and $(CH_2)_3NH_2PbI_3$.

Formability of inorganic perovskite structures can be rationalized via geometrical factors such as the Goldschmidt's tolerance factor[19] and Pauling's octahedral factor.[20] To

Received: November 23, 2017
Accepted: February 1, 2018
Published: February 1, 2018

DOI: 10.1021/acs.jpclett.7b03114
J. Phys. Chem. Lett. 2018, 9, 874−880

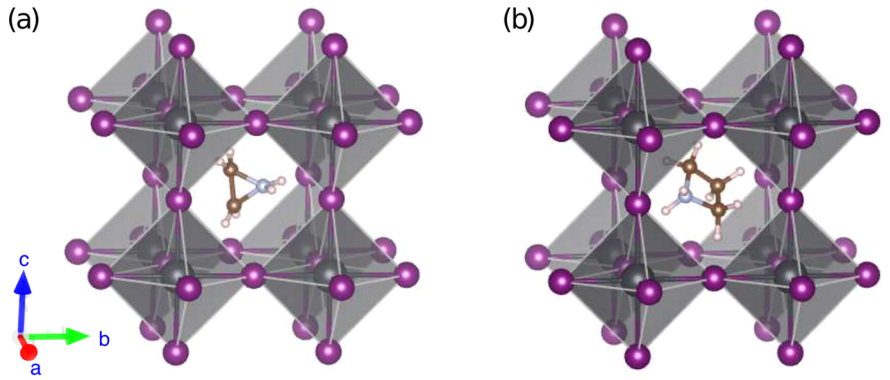

Figure 1. Quasicubic crystal structures of cyclic ring-based perovskites: (a) aziridinium lead iodide$(CH_2)_2NH_2PbI_3$ and (b) azetidinium lead iodide $(CH_2)_3NH_2PbI_3$.

calculate the geometrical factors of hybrid halide perovskites, the effective organic cation radii are estimated as proposed by Kieslich et al.[16] The effective radii of three- and four-membered ring cations are listed in Table 1 along the side with the

Table 1. Geometrical Factors of Selected Perovskites and Calculated Ionization Energies of Corresponding *A* Site Cations

			ionization energy (eV)	
radical *A*	A^+ cation radius (pm)	tolerance factor for $APbI_3$	DFT[a]	exp.
Cs	181	0.81	3.85	3.89[23]
CH_3NH_3	215	0.91	4.36	4.30 ± 0.1[24]
$(CH_2)_2NH_2$	227	0.93	4.07	
$(CH_2)_3NH_2$	250	0.98	3.96	
$HC(NH_2)_2$	264	1.01	4.18	

[a]Ionization energies are obtained from the DFT−PBE (Perdew−Burke−Ernzerhof)[21] total energy difference of cations and neutral radicals including the vibrational zero-point energy.

representative organic and inorganic cations. The size of cyclic cations is between that of CH_3NH_3 and $HC(NH_2)_2$. The cation effective radii are used to evaluate the Goldschmidt's tolerance factor t for $APbI_3$ perovskite structures (Table 1). The tolerance factor of $(CH_2)_3NH_2PbI_3$ is too large to form a cubic or tetragonal structure ($t > 0.96$[22]), whereas the tolerance factor for $(CH_2)_2NH_2PbI_3$ is within the perovskite formability limits.

According to our previous study,[15] the radical ionization energy at *A* site has an effect on the final reaction enthalpy of hybrid halide perovskites. The lower ionization energy, the more stable is the structure. Results in Table 1 demonstrate that both radicals $(CH_2)_2NH_2$ and $(CH_2)_3NH_2$ have lower ionization energies than MA. Their values are close to the ionization energy of Cs, which is the lowest one in the periodic table. This result suggests that $(CH_2)_2NH_2PbI_3$ and $(CH_2)_3NH_2PbI_3$ should be more stable than $CH_3NH_3PbI_3$.

To further investigate the stability of $(CH_2)_2NH_2PbI_3$, we use the following decomposition reaction equation

$$(CH_2)_2NH_2PbI_3 \rightarrow (CH_2)_2NH_2I + PbI_2 \quad (1)$$

and the corresponding enthalpy

$$\Delta H_r = E_{tot}[(CH_2)_2NH_2PbI_3] - E_{tot}[(CH_2)_2NH_2I] - E_{tot}[PbI_2] \quad (2)$$

The total energies E_{tot} of products and the reactant are evaluated using DFT. If the total energy of the products is lower than the total energy of the reactant, the perovskite structure is deemed unstable.[9] This approach ignores finite temperature components of the free energy, which is on the order of −0.1 eV for $CH_3NH_3PbI_3$.[25]

As a benchmark, we analyzed the stability and polymorphism of $CH_3NH_3PbI_3$. Among various polymorphs, we include a possibility for a hexagonal phase because perovskite structures with large cations ($t > 0.96$) have a tendency to adapt a hexagonal structure. PBE is first used as the exchange-correlation functional. Results listed in Table 2 suggest that the hexagonal structure of $CH_3NH_3PbI_3$ has the lowest total energy at 0 K. This finding contradicts experimental data,[26−28] according to which $CH_3NH_3PbI_3$ adapts the orthorhombic

Table 2. Polymorphism of Hybrid Halide Perovskites Predicted Using DFT with and without the van der Waals Correction

		PBE		PBE+vdW(D3)	
compound	phase	E_{tot} (meV)	ΔH_r (meV)	E_{tot} (meV)	ΔH_r (meV)
$CH_3NH_3PbI_3$	cubic	111	71	122	160
	tetragonal	79	39	44	82
	orthorhombic	58	18	0	38
	hexagonal	0	−40	11	49
$(CH_2)_2NH_2PbI_3$	cubic	107	−44	67	−81
	tetragonal	141	−10	54	−93
	orthorhombic	140	−12	63	−84
	hexagonal	0	−151	0	−147
$(CH_2)_3NH_2PbI_3$	cubic	174	−51	73	−199
	tetragonal	194	−31	99	−173
	orthorhombic	171	−54	71	−201
	hexagonal	0	−225	0	−272
$HC(NH_2)_2PbI_3$	cubic	296	179	238	266
	tetragonal	142	25	50	79
	orthorhombic	113	−4	32	61
	hexagonal	0	−117	0	29
$CH_3NH_3PbBr_3$	cubic			71	13
	orthorhombic			0	−58
$CH_3NH_3PbCl_3$	cubic			68	−41
	orthorhombic			0	−109

DOI: 10.1021/acs.jpclett.7b03114
J. Phys. Chem. Lett. 2018, 9, 874−880

structure below 162.2 K. Recently, a theory-based study reported similar controversial results on the hexagonal $CH_3NH_3PbI_3$ to have the lowest total energy and predicted it as a stable low-temperature phase.[29] However, we are inclined to think that the hexagonal phase of $CH_3NH_3PbI_3$ is probably a metastable phase. It is the choice of the exchange-correlation functional that is a possible reason for DFT failure to accurately predict the correct polymorphism transformation order of $CH_3NH_3PbI_3$. Thus different exchange-correlation functionals are employed to evaluate the polymorphism transformation of $CH_3NH_3PbI_3$ (see Figure 2).

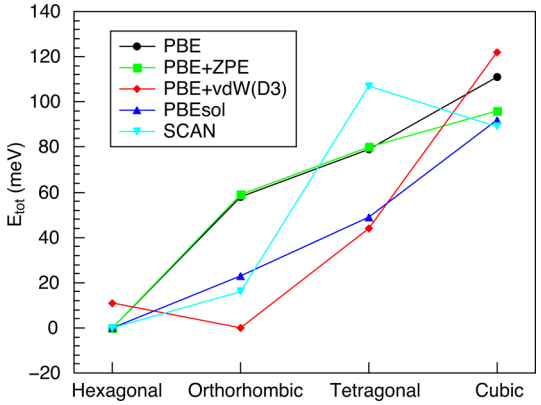

Figure 2. Polymorphism of $CH_3NH_3PbI_3$ with different exchange-correlation functionals. The origin of the energy scale is set at the lowest energy structure for each computational technique used.

Figure 2 illustrates the total energies of different phases of $CH_3NH_3PbI_3$ obtained using PBE, PBE+ZPE (zero-point energy correction), PBE+vdW(D3),[30] PBEsol,[31,32] and SCAN[33] exchange-correlation functionals. Bokdam et al.[34] proposed SCAN as the superior exchange-correlation functional for structural simulations of hybrid halide perovskites. However, all methods except for the PBE+vdW(D3) favor the hexagonal structure at low temperature. The result indicates the importance of dispersion interactions to stabilize the low-temperature orthorhombic $CH_3NH_3PbI_3$. Li and Rinke[35] pointed out that the van der Waals (vdW) correction is also essential to obtain an accurate lattice constant of hybrid halide perovskites. It should be noted that Thind et al.[29] performed similar calculations including vdW correction, and their results showed that the hexagonal phase still has the lowest total energy among all of the phases, which contradicts our results. We suspect that the reason for discrepancy can be a suboptimal structure of the orthorhombic phase used by Thind et al.[29]

Because van der Waals effects are important for the polymorphism of $CH_3NH_3PbI_3$, the same can be extended for other types of hybrid halide perovskites. Thus we focus on results obtained with PBE+vdW(D3) exchange-correlation functional in the remaining part of the paper. Table 2 lists the results of polymorphism prediction and corresponding decomposition reaction enthalpies for the perovskites of interest here. It is noticed that except for $CH_3NH_3PbI_3$, all of the other perovskites favor the hexagonal structures as the low-temperature stable phase. This trend can be attributed to a greater size of organic cations involved. For $CH_3NH_3PbI_3$ and $HC(NH_2)_2PbI_3$, ΔH_r values are weakly positive, which contradicts formability of those compounds. The final temperature contribution will lower the free energy by ∼0.1 eV,[25] making their formability feasible.

Recent comparative studies of stability among $CH_3NH_3PbX_3$ perovskites with X = Cl, Br, and I reported that a higher stability can be achieved by switching halide from I to Br and Cl.[8,9,36−39] Our calculated stability trend of $CH_3NH_3PbX_3$ is consistent with those observations. The lower reaction enthalpies of $(CH_2)_2NH_2PbI_3$ suggest that the stability of $(CH_2)_2NH_2PbI_3$ will be superior to $CH_3NH_3PbCl_3$ (Table 2).

Moreover, Tenuta et al.[25] indicated that the degradation of $APbI_3$ perovskites in the moist environment is governed by the solubility of a AI salt. The saturation concentration c_s of AI in the solvent exponentially depends on the reaction enthalpy given by eq 2. Considering a low reaction enthalpy of $(CH_2)_3NH_2PbI_3$, its decomposition via solvation of $(CH_2)_3NH_2I$ in water will be hindered. This prediction is consistent with the exceptional moisture stability of $(CH_2)_3NH_2PbI_3$.[17]

The solubility of AI_m salts can be captured by evaluating an enthalpy of the following reaction

$$AI_m(s) \rightarrow A^{m+}(aq) + mI^-(aq) \quad (3)$$

Energies of the corresponding products are evaluated using implicit solvation model of VASPsol[40,41] and the solvation enthalpies are presented in Table 3. The lower enthalpy favors solubility of the salt. The high solubility of CH_3NH_3I in water and the low solubility of PbI_2 correlate with the enthalpy values listed in Table 3. The four discussed AI salts have similar solvation enthalpies ranging from 0.35 to 0.45 eV. It suggests a similar solubilities of the AI salts. Therefore, the proposed perovskite $(CH_2)_2NH_2PbI_3$ should be less prone to decomposition via dissolution in water due to its higher decomposition reaction enthalpy (Table 2) rather than differences in solubility of the salt.

Table 3. Solvation Enthalpy ΔH of Iodide Salts in Water

salt	ΔH (eV)
CH_3NH_3I	0.45
$(CH_2)_2NH_2I$	0.45
$(CH_2)_3NH_2I$	0.39
$HC(NH_2)_2I$	0.35
PbI_2	2.38

We compared the stability of the proposed cation with other mainstream cations using the following decomposition pathway, taking $(CH_2)_2NH_2^+$ as an example

$$(CH_2)_2NH_2^+(aq) + I^-(aq) \rightarrow (CH_2)_2NH(g) + HI(g) \quad (4)$$

The corresponding enthalpies are listed in Table 4. Positive enthalpies indicate the discussed four cations are stable in an aqueous solution.

Table 4. Decomposition Enthalpy of Cations via a Proton-Exchange Reaction (eq 4)

cation A^+	ΔH (eV)
$CH_3NH_3^+$	1.47
$(CH_2)_2NH_2^+$	1.25
$(CH_2)_3NH_2^+$	1.42
$HC(NH_2)_2^+$	1.89

DOI: 10.1021/acs.jpclett.7b03114
J. Phys. Chem. Lett. 2018, 9, 874−880

For the photovoltaic application of $(CH_2)_2NH_2PbI_3$, it is crucial that its structure adapts a cubic phase at room temperature. The Goldschmidt's tolerance factors of $(CH_2)_2NH_2PbI_3$ and $CH_3NH_3PbBr_3$ are the same, 0.93.[36] Because $CH_3NH_3PbBr_3$ prefers a cubic structure at the room temperature,[26,27] we can expect that $(CH_2)_2NH_2PbI_3$ will exhibit a similar polymorphism as a function of temperature. Besides, we found that the high-temperature phase transition point versus the energy difference between the low-temperature and high-temperature phases follows a linear trend (see Figure 3). From Figure 3, energy difference between cubic and hexagonal structures of $(CH_2)_2NH_2PbI_3$ is 67 meV, which is close to the energy difference of 68 meV between cubic and orthorhombic structures of $CH_3NH_3PbCl_3$. The tetragonal $CH_3NH_3PbCl_3$ transits to a cubic phase at 190 K. We expect $(CH_2)_2NH_2PbI_3$ to have similar transition behavior and to adapt the cubic phase above 190 K.

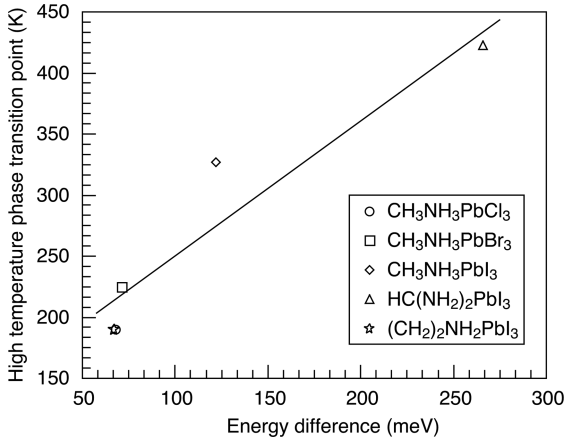

Figure 3. Correlation between the high-temperature phase-transition point and the energy difference between the low-temperature phase and high-temperature phase. The linear line is a guide to the eye. High-temperature transition temperatures are taken from refs 26, 27, and 42.

Until now, we found that the $(CH_2)_2NH_2PbI_3$ perovskite solar cells should be more stable than $CH_3NH_3PbI_3$ and $HC(NH_2)_2PbI_3$. The key question that remains unanswered is whether the proposed perovskite structure can serve as a solar cell absorber material. Here we report the band gap for the hypothetical $(CH_2)_2NH_2PbI_3$ obtained on the framework of *GW* approximation, taking into account relativistic effects. It is known that band gap is sensitive to the structural properties. We found that the PBE+vdW(D3), PBEsol, and SCAN exchange-correlation functionals can provide an accurate prediction for the lattice constants (see the Supporting Information). Here we continue to use PBE+vdW(D3) optimized perovskite structures to remain consistent with the section on stability calculations. Results for band gaps obtained using PBE+vdW(D3) exchange-correlation functional with and without the spin-orbit coupling (SOC) are shown in Table 5.

It is well known that DFT calculations with SOC grossly underestimate the band gap of perovskites.[43] In Table 5, the calculated band gaps with PBE+vdW(D3)+SOC are ~1 eV lower than the result without SOC. Band gaps increase from cubic phase to hexagonal phase. Polymorphs of $(CH_2)_3NH_2PbI_3$ demonstrate the largest band gaps among the four perovskites studied here. Band gaps of different phases of $(CH_2)_2NH_2PbI_3$ lie between $CH_3NH_3PbI_3$ and $HC(NH_2)_2PbI_3$. It is obvious that hexagonal phases show much large band gaps than perovskite phases. Thus the hexagonal phase around room temperature is not desirable when aiming at photovoltaic applications.

Figure 4 shows a relativistic band structure of quasicubic $(CH_2)_2NH_2PbI_3$. The fundamental band gap is near R-point of the Brillouin zone. The presence of a Rashba splitting is noticeable at the vicinity of the band extrema; however, its magnitude is heavily reduced when compared with the Rashba splitting at the $CH_3NH_3PbI_3$ band edges.[44−47] The Rashba splitting in hybrid halide perovskites originates from the strong spin−orbit interaction and distortions in the Pb-centered octahedron.[46,47] A more centrosymmetric PbI_3 cage of the quasicubic structure and its larger volume can be a reason for the reduced Rashba splitting in $(CH_2)_2NH_2PbI_3$.

The Rashba splitting in hybrid halide perovskites introduces an effectively indirect band gap, which prolongs the carrier lifetime.[46,48] We expect the reduced Rashba splitting in $(CH_2)_2NH_2PbI_3$ not to impede its power conversion efficiency for photovoltaic applications, because a similar weak splitting can be found in the band structures of $HC(NH_2)_2PbI_3$.[49]

Table 5. Band Gaps (eV) of Hybrid Halide Perovskites Prediction with PBE+vdW(D3) and PBE+vdW(D3)+SOC

compound	phase	PBE+vdW(D3)	PBE+vdW(D3)+SOC
$CH_3NH_3PbI_3$	cubic	1.44	0.38
	tetragonal	1.51	0.76
	orthorhombic	1.72	0.86
	hexagonal	2.53	2.20
$(CH_2)_2NH_2PbI_3$	cubic	1.35	0.36
	tetragonal	1.58	0.62
	orthorhombic	1.53	0.58
	hexagonal	2.74	2.35
$(CH_2)_3NH_2PbI_3$	cubic	1.56	0.54
	tetragonal	1.61	0.64
	orthorhombic	1.71	0.67
	hexagonal	2.69	2.31
$HC(NH_2)_2PbI_3$	cubic	1.34	0.33
	tetragonal	1.60	0.67
	orthorhombic	1.66	0.67
	hexagonal	2.52	2.20

DOI: 10.1021/acs.jpclett.7b03114
J. Phys. Chem. Lett. 2018, 9, 874−880

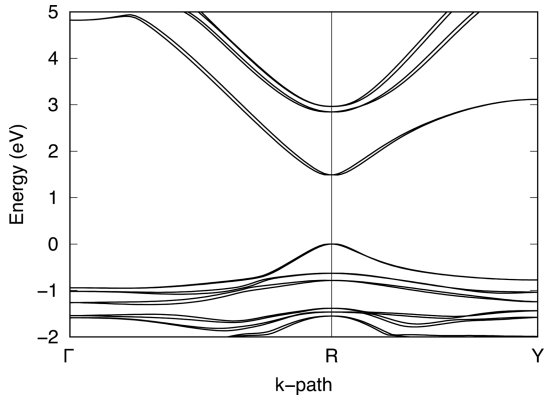

Figure 4. Electronic band structure of $(CH_2)_2NH_2PbI_3$ calculated at the PBE+SOC level with the band gap adjusted to match the G_0W_0+SOC result in Table 6. The *k* path includes the following high-symmetry points: Γ(0,0,0), R(0.5,0.5,0.5), and Y(0,0.5,0).

Recently, Yang et al.[5] fabricated formamidinium-lead-halide-based perovskite solar cells with a certified 22.1% power conversion efficiency.

It is well known that a first-principles *GW* approximation with SOC can accurately predict the band gaps of hybrid halide perovskites.[43,45] First, we used a single-shot G_0W_0 approximation with SOC to evaluate the band gaps of quasicubic phases for perovskites of interest (Table 6). Next, we carried out a partially self-consistent calculation by performing four iterations of *G* only (referred to as GW_0). The single-shot G_0W_0 method gave the best match of band gaps with the experimental values (Table 6). On the basis of this Table, we found that the band gap of quasicubic $(CH_2)_2NH_2PbI_3$ is 0.17 eV lower than quasicubic $CH_3NH_3PbI_3$ and 0.09 eV higher than quasicubic $HC(NH_2)_2PbI_3$. This result suggests that $(CH_2)_2NH_2PbI_3$ may offer a superior utilization of the Sun's spectrum than $CH_3NH_3PbI_3$.

To summarize, we used first-principles calculations to predict structure and characterize stability and electronic properties of hybrid halide perovskites. The PBE exchange-correlation functional was used to evaluate the ionization energy of different cations. The polymorphism of perovskites is best captured when van der Waals correction is included at the PBE+vdW(D3) level to accurately predict the order of phases. An implicit solvation model was used to describe the interaction between a solute and solvent (water) when evaluating solubility of perovskite decomposition products. The electronic band structure and Rashba splitting effect are captured through a relativistic calculation at the PBE level. To estimate the band gaps of perovskites, we used a quasiparticle *GW* approximation considering the spin−orbit interaction, which gives the most accurate results compared with experimental data. As a result, we proposed a three-membered cyclic organic cation-based hybrid halide perovskite $(CH_2)_2NH_2PbI_3$, which has a potential to be used as the absorber material for photovoltaics. The low ionization energy of organic radical $(CH_2)_2NH_2$ decreases the reaction enthalpy of forming the corresponding perovskite. It suggests that this lower reaction enthalpy renders a much better stability of $(CH_2)_2NH_2PbI_3$ than $CH_3NH_3PbI_3$ and $HC(NH_2)_2PbI_3$. The appropriate cation radius of $(CH_2)_2NH_2$ for the PbI_3 framework and a low-energy difference between high-temperature and low-temperature phases make $(CH_2)_2NH_2PbI_3$ transfer to a cubic phase feasible below the room temperature. Relativistic band structure plot demonstrates the existence of a Rashba splitting in $(CH_2)_2NH_2PbI_3$, albeit less prominent than in $CH_3NH_3PbI_3$. The Rashba splitting will allow $(CH_2)_2NH_2PbI_3$ to form an indirect band gap near R-point in the Brillouin zone and benefit from an enhanced charge-carrier lifetime. *GW* calculations suggest that the cubic phase of $(CH_2)_2NH_2PbI_3$ has an even lower band gap of 1.49 eV than $CH_3NH_3PbI_3$, thereby making the former perovskite a suitable absorber material for solar cells.

■ ASSOCIATED CONTENT

Supporting Information

The Supporting Information is available free of charge on the ACS Publications website at DOI: 10.1021/acs.jpclett.7b03114. Crystallographic information files (CIF) with atomic structures used in calculations can be accessed through the Cambridge crystallographic data center (CCDC deposition numbers 1584308-1584327).

Computational details and lattice constants prediction (PDF)

■ AUTHOR INFORMATION

Corresponding Authors

*C.Z.: E-mail: zhengc8@mcmaster.ca. Tel: +1647-936-1436.
*O.R.: E-mail: rubelo@mcmaster.ca. Tel: +1905-525-9140, ext. 24094.

ORCID

Chao Zheng: 0000-0001-5441-6720
Oleg Rubel: 0000-0001-5104-5602

Notes

The authors declare no competing financial interest.

■ ACKNOWLEDGMENTS

Funding was provided by the Natural Sciences and Engineering Research Council of Canada under the Discovery Grant Program RGPIN-2015-04518. The work was performed using a Compute Canada infrastructure.

■ REFERENCES

(1) Kojima, A.; Teshima, K.; Shirai, Y.; Miyasaka, T. Organometal Halide Perovskites as Visible-Light Sensitizers for Photovoltaic Cells. *J. Am. Chem. Soc.* **2009**, *131*, 6050−6051.
(2) Kim, H. S.; Lee, C. R.; Im, J. H.; Lee, K. B.; Moehl, T.; Marchioro, A.; Moon, S. J.; Humphry Baker, R.; Yum, J. H.; Moser, J. E.; et al. Lead Iodide Perovskite Sensitized All-Solid-State Submicron

Table 6. Quasiparticle Band Gaps (eV) of Various Perovskites in the Quasicubic Phase

perovskites	G_0W_0+SOC	GW_0+SOC	exp.	reported *GW*+SOC
$CH_3NH_3PbI_3$	1.66	1.76	1.69[50]	1.27−1.67[45,50−53]
$(CH_2)_2NH_2PbI_3$	1.49	1.53		
$(CH_2)_3NH_2PbI_3$	1.84	1.99		
$HC(NH_2)_2PbI_3$	1.40	1.44	1.43−1.48[42,54−56]	1.46[57]

DOI: 10.1021/acs.jpclett.7b03114
J. Phys. Chem. Lett. 2018, 9, 874−880

Thin Film Mesoscopic Solar Cell with Efficiency Exceeding 9%. *Sci. Rep.* **2012**, *2*, 591.
(3) Lee, M. M.; Teuscher, J.; Miyasaka, T.; Murakami, T. N.; Snaith, H. J. Efficient Hybrid Solar Cells Based on Meso-Superstructured Organometal Halide Perovskites. *Science* **2012**, *338*, 643−647.
(4) Eperon, G. E.; Burlakov, V. M.; Docampo, P.; Goriely, A.; Snaith, H. J. Morphological Control for High Performance, Solution-Processed Planar Heterojunction Perovskite Solar Cells. *Adv. Funct. Mater.* **2014**, *24*, 151−157.
(5) Yang, W. S.; Park, B.-W.; Jung, E. H.; Jeon, N. J.; Kim, Y. C.; Lee, D. U.; Shin, S. S.; Seo, J.; Kim, E. K.; Noh, J. H.; et al. Iodide Management in Formamidinium-Lead-Halide-Based Perovskite Layers for Efficient Solar Cells. *Science* **2017**, *356*, 1376−1379.
(6) Christians, J. A.; Miranda Herrera, P. A.; Kamat, P. V. Transformation of the Excited State and Photovoltaic Efficiency of $CH_3NH_3PbI_3$ Perovskite upon Controlled Exposure to Humidified Air. *J. Am. Chem. Soc.* **2015**, *137*, 1530−1538.
(7) Wozny, S.; Yang, M.; Nardes, A. M.; Mercado, C. C.; Ferrere, S.; Reese, M. O.; Zhou, W.; Zhu, K. Controlled Humidity Study on the Formation of Higher Efficiency Formamidinium Lead Triiodide-Based Solar Cells. *Chem. Mater.* **2015**, *27*, 4814−4820.
(8) Buin, A.; Comin, R.; Xu, J.; Ip, A. H.; Sargent, E. H. Halide-Dependent Electronic Structure of Organolead Perovskite Materials. *Chem. Mater.* **2015**, *27*, 4405−4412.
(9) Zhang, Y. Y.; Chen, S.; Xu, P.; Xiang, H.; Gong, X. G.; Walsh, A.; Wei, S. H. Intrinsic Instability of the Hybrid Halide Perovskite Semiconductor $CH_3NH_3PbI_3$. 2015, arXiv:1506.01301. arXiv.org e-Print archive. https://arxiv.org/abs/1506.01301.
(10) Kohn, W.; Sham, L. J. Self-Consistent Equations including Exchange and Correlation Effects. *Phys. Rev.* **1965**, *140*, A1133.
(11) Im, J. H.; Lee, C. R.; Lee, J. W.; Park, S. W.; Park, N. G. 6.5% Efficient Perovskite Quantum-Qot-Sensitized Solar Cell. *Nanoscale* **2011**, *3*, 4088−4093.
(12) Gevorgyan, S. A.; Madsen, M. V.; Dam, H. F.; Jørgensen, M.; Fell, C. J.; Anderson, K. F.; Duck, B. C.; Mescheloff, A.; Katz, E. A.; Elschner, A.; et al. Interlaboratory Outdoor Stability Studies of Flexible Roll-to-Roll Coated Organic Photovoltaic Modules: Stability over 10,000 h. *Sol. Energy Mater. Sol. Cells* **2013**, *116*, 187−196.
(13) Zhou, H.; Chen, Q.; Li, G.; Luo, S.; Song, T. B.; Duan, H. S.; Hong, Z.; You, J.; Liu, Y.; Yang, Y. Interface Engineering of Highly Efficient Perovskite Solar Cells. *Science* **2014**, *345*, 542−546.
(14) Chauhan, A.; Kumar, P. Degradation in Perovskite Solar Cells Stored in Different Environmental Conditions. *J. Phys. D: Appl. Phys.* **2017**, *50*, 325105−325116.
(15) Zheng, C.; Rubel, O. Ionization Energy as a Stability Criterion for Halide Perovskites. *J. Phys. Chem. C* **2017**, *121*, 11977−11984.
(16) Kieslich, G.; Sun, S.; Cheetham, A. K. Solid-State Principles Applied to Organic-Inorganic Perovskites: New Tricks for an Old Dog. *Chem. Sci.* **2014**, *5*, 4712−4715.
(17) Pering, S. R.; Deng, W.; Troughton, J. R.; Kubiak, P. S.; Ghosh, D.; Niemann, R. G.; Brivio, F.; Jeffrey, F. E.; Walker, A. B.; Islam, M. S.; et al. Azetidinium Lead Iodide for Perovskite Solar Cells. *J. Mater. Chem. A* **2017**, *5*, 20658−20665.
(18) Solka, B.; Russell, M. Energetics of Formation of Some Structural Isomers of Gaseous $[C_2H_5O]^+$ and $[C_2H_6N]^+$ ions. *J. Phys. Chem.* **1974**, *78*, 1268−1273.
(19) Goldschmidt, V. M. Die Gesetze der Krystallochemie. *Naturwissenschaften* **1926**, *14*, 477−485.
(20) Pauling, L. The Principles Determining the Structure of Complex Ionic Crystals. *J. Am. Chem. Soc.* **1929**, *51*, 1010−1026.
(21) Perdew, J. P.; Burke, K.; Ernzerhof, M. Generalized Gradient Approximation Made Simple. *Phys. Rev. Lett.* **1996**, *77*, 3865−3868.
(22) Feng, L.; Jiang, L.; Zhu, M.; Liu, H.; Zhou, X.; Li, C. Formability of ABO_3 Cubic Perovskites. *J. Phys. Chem. Solids* **2008**, *69*, 967−974.
(23) Moore, C. E. *Ionization Potentials and Ionization Limits Derived from the Analyses of Optical Spectra*; United States Government Printing Office: Washington, DC, 1970.
(24) Jeon, S. J.; Raksit, A. B.; Gellene, G. I.; Porter, R. F. Formation of Hypervalent Ammoniated Radicals by Neutralized Ion Beam Techniques. *J. Am. Chem. Soc.* **1985**, *107*, 4129−4133.
(25) Tenuta, E.; Zheng, C.; Rubel, O. Thermodynamic Origin of Instability in Hybrid Halide Perovskites. *Sci. Rep.* **2016**, *6*, 37654.
(26) Poglitsch, A.; Weber, D. Dynamic Disorder in Methylammoniumtrihalogenoplumbates (II) Observed by Millimeter-Eave Spectroscopy. *J. Chem. Phys.* **1987**, *87*, 6373−6378.
(27) Onoda-Yamamuro, N.; Matsuo, T.; Suga, H. Calorimetric and IR Spectroscopic Studies of Phase Transitions in Methylammonium Trihalogenoplumbates (II). *J. Phys. Chem. Solids* **1990**, *51*, 1383−1395.
(28) Whitfield, P.; Herron, N.; Guise, W.; Page, K.; Cheng, Y.; Milas, I.; Crawford, M. Structures, Phase Transitions and Tricritical Behavior of the Hybrid Perovskite Methyl Ammonium Lead Iodide. *Sci. Rep.* **2016**, *6*, 35685.
(29) Thind, A. S.; Huang, X.; Sun, J.; Mishra, R. First-Principles Prediction of a Stable Hexagonal Phase of $CH_3NH_3PbI_3$. *Chem. Mater.* **2017**, *29*, 6003−6011.
(30) Grimme, S.; Antony, J.; Ehrlich, S.; Krieg, H. A Consistent and Accurate *Ab Initio* Parametrization of Density Functional Dispersion Correction (DFT-D) for the 94 Elements H-Pu. *J. Chem. Phys.* **2010**, *132*, 154104.
(31) Perdew, J. P.; Ruzsinszky, A.; Csonka, G. I.; Vydrov, O. A.; Scuseria, G. E.; Constantin, L. A.; Zhou, X.; Burke, K. Restoring the Density-Gradient Expansion for Exchange in Solids and Surfaces. *Phys. Rev. Lett.* **2008**, *100*, 136406.
(32) Csonka, G. I.; Perdew, J. P.; Ruzsinszky, A.; Philipsen, P. H. T.; Lebègue, S.; Paier, J.; Vydrov, O. A.; Ángyán, J. G. Assessing the Performance of Recent Density Functionals for Bulk Solids. *Phys. Rev. B: Condens. Matter Mater. Phys.* **2009**, *79*, 155107.
(33) Sun, J.; Ruzsinszky, A.; Perdew, J. P. Strongly Constrained and Appropriately Normed Semilocal Density Functional. *Phys. Rev. Lett.* **2015**, *115*, 036402.
(34) Bokdam, M.; Lahnsteiner, J.; Ramberger, B.; Schäfer, T.; Kresse, G. Assessing Density Functionals Using Many Body Theory for Hybrid Perovskites. *Phys. Rev. Lett.* **2017**, *119*, 145501.
(35) Li, J.; Rinke, P. Atomic Structure of Metal-Halide Perovskites from First-Principles: The Chicken-and-Egg Paradox of the Organic-Inorganic Interaction. *Phys. Rev. B: Condens. Matter Mater. Phys.* **2016**, *94*, 045201.
(36) Nagabhushana, G.; Shivaramaiah, R.; Navrotsky, A. Direct Calorimetric Verification of Thermodynamic Instability of Lead Halide Hybrid Perovskites. *Proc. Natl. Acad. Sci. U. S. A.* **2016**, *113*, 7717−7721.
(37) Jong, U. G.; Yu, C. J.; Ri, J. S.; Kim, N. H.; Ri, G. C. Influence of Halide Composition on the Structural, Electronic, and Optical Properties of Mixed $CH_3NH_3Pb(I_{1-x}Br_x)_3$ Perovskites Calculated using the Virtual Crystal Approximation Method. *Phys. Rev. B: Condens. Matter Mater. Phys.* **2016**, *94*, 125139.
(38) Mali, S. S.; Shim, C. S.; Hong, C. K. Highly Stable and Efficient Solid-State Solar Cells Based on Methylammonium Lead Bromide ($CH_3NH_3PbBr_3$) Perovskite Quantum Dots. *NPG Asia Mater.* **2015**, *7*, e208.
(39) Maculan, G.; Sheikh, A. D.; Abdelhady, A. L.; Saidaminov, M. I.; Haque, M. A.; Murali, B.; Alarousu, E.; Mohammed, O. F.; Wu, T.; Bakr, O. M. $CH_3NH_3PbCl_3$ Single Crystals: Inverse Temperature Crystallization and Visible-Blind UV-Photodetector. *J. Phys. Chem. Lett.* **2015**, *6*, 3781−3786.
(40) Mathew, K.; Sundararaman, R.; Letchworth-Weaver, K.; Arias, T.; Hennig, R. G. Implicit Solvation Model for Density-Functional Study of Nanocrystal Surfaces and Reaction Pathways. *J. Chem. Phys.* **2014**, *140*, 084106.
(41) Mathew, K.; Hennig, R. G. Implicit Self-Consistent Description of Electrolyte in Plane-Wave Density-Functional Theory. 2016, arXiv:1601.03346. arXiv.org e-Print archive. https://arxiv.org/abs/1601.03346.
(42) Koh, T. M.; Fu, K.; Fang, Y.; Chen, S.; Sum, T.; Mathews, N.; Mhaisalkar, S. G.; Boix, P. P.; Baikie, T. Formamidinium-Containing

DOI: 10.1021/acs.jpclett.7b03114
J. Phys. Chem. Lett. 2018, 9, 874−880

Metal-Halide: An Alternative Material for Near-IR Absorption Perovskite Solar Cells. *J. Phys. Chem. C* **2014**, *118*, 16458−16462.
(43) Umari, P.; Mosconi, E.; De Angelis, F. Relativistic GW Calculations on $CH_3NH_3PbI_3$ and $CH_3NH_3SnI_3$ Perovskites for Solar Cell Applications. *Sci. Rep.* **2015**, *4*, 4467.
(44) Even, J.; Pedesseau, L.; Jancu, J. M.; Katan, C. Importance of Spin-Orbit Coupling in Hybrid Organic/Inorganic Perovskites for Photovoltaic Applications. *J. Phys. Chem. Lett.* **2013**, *4*, 2999−3005.
(45) Brivio, F.; Butler, K. T.; Walsh, A.; van Schilfgaarde, M. Relativistic Quasiparticle Self-Consistent Electronic Structure of Hybrid Halide Perovskite Photovoltaic Absorbers. *Phys. Rev. B: Condens. Matter Mater. Phys.* **2014**, *89*, 155204.
(46) Zheng, F.; Tan, L. Z.; Liu, S.; Rappe, A. M. Rashba Spin-Orbit Coupling Enhanced Carrier Lifetime in $CH_3NH_3PbI_3$. *Nano Lett.* **2015**, *15*, 7794−7800.
(47) Rubel, O.; Bokhanchuk, A. Robust Bloch Character at the Band Edges of Hybrid Halide perovskites. 2015, arXiv:1508.03612. arXiv.org e-Print archive. https://arxiv.org/abs/1508.03612.
(48) Stier, A. V.; McCreary, K. M.; Jonker, B. T.; Kono, J.; Crooker, S. A. Exciton Diamagnetic Shifts and Valley Zeeman Effects in Monolayer WS_2 and MoS_2 to 65 T. *Nat. Commun.* **2016**, *7*, 10643.
(49) Chen, T.; Chen, W. L.; Foley, B. J.; Lee, J.; Ruff, J. P.; Ko, J. P.; Brown, C. M.; Harriger, L. W.; Zhang, D.; Park, C.; et al. Origin of Long Lifetime of Band-Edge Charge Carriers in Organic-Inorganic Lead Iodide Perovskites. *Proc. Natl. Acad. Sci. U. S. A.* **2017**, *114*, 7519−7524.
(50) Quarti, C.; Mosconi, E.; Ball, J. M.; D'Innocenzo, V.; Tao, C.; Pathak, S.; Snaith, H. J.; Petrozza, A.; De Angelis, F. Structural and Optical Properties of Methylammonium Lead Iodide across the Tetragonal to Cubic Phase Transition: Implications for Perovskite Solar Cells. *Energy Environ. Sci.* **2016**, *9*, 155−163.
(51) Ahmed, T.; Salim, T.; La-o vorakiat, C.; Lam, Y.; Chia, E. E.; Zhu, J. X.; et al. Optical Properties of Organometallic Perovskite: An *Ab Initio* Study using Relativistic GW Correction and Bethe-Salpeter Equation. *EPL* **2014**, *108*, 67015.
(52) Bokdam, M.; Sander, T.; Stroppa, A.; Picozzi, S.; Sarma, D.; Franchini, C.; Kresse, G. Role of Polar Phonons in the Photo Excited State of Metal Halide Perovskites. *Sci. Rep.* **2016**, *6*, 28618.
(53) Gao, W.; Gao, X.; Abtew, T. A.; Sun, Y. Y.; Zhang, S.; Zhang, P. Quasiparticle Band Gap of Organic-Inorganic Hybrid Perovskites: Crystal Structure, Spin-Orbit Coupling, and Self-Energy Effects. *Phys. Rev. B: Condens. Matter Mater. Phys.* **2016**, *93*, 085202.
(54) Pang, S.; Hu, H.; Zhang, J.; Lv, S.; Yu, Y.; Wei, F.; Qin, T.; Xu, H.; Liu, Z.; Cui, G. $NH_2CH = NH_2PbI_3$: An Alternative Organolead Iodide Perovskite Sensitizer for Mesoscopic Solar Cells. *Chem. Mater.* **2014**, *26*, 1485−1491.
(55) Eperon, G. E.; Stranks, S. D.; Menelaou, C.; Johnston, M. B.; Herz, L. M.; Snaith, H. J. Formamidinium Lead Trihalide: A Broadly Tunable Perovskite for Efficient Planar Heterojunction Solar Cells. *Energy Environ. Sci.* **2014**, *7*, 982−988.
(56) Stoumpos, C. C.; Kanatzidis, M. G. The Renaissance of Halide Perovskites and Their Evolution as Emerging Semiconductors. *Acc. Chem. Res.* **2015**, *48*, 2791−2802.
(57) Arora, N.; Orlandi, S.; Dar, M. I.; Aghazada, S.; Jacopin, G.; Cavazzini, M.; Mosconi, E.; Gratia, P.; De Angelis, F.; Pozzi, G.; et al. High Open-Circuit Voltage: Fabrication of Formamidinium Lead Bromide Perovskite Solar Cells using Fluorene-Dithiophene Derivatives as Hole-Transporting Materials. *ACS Energy Lett.* **2016**, *1*, 107−112.

DOI: 10.1021/acs.jpclett.7b03114
J. Phys. Chem. Lett. 2018, 9, 874−880